POLITECNICO DI TORINO
Repository ISTITUZIONALE

A cascade approach for the early detection and localization of myocardial infarction in 2D-echocardiography

Original
A cascade approach for the early detection and localization of myocardial infarction in 2D-echocardiography / Gomez, C., Letizia, A., Tufano, V., Molinari, F., Salvi, M.. - In: MEDICAL ENGINEERING & PHYSICS. - ISSN 1350-4533. - 143:(2025). [10.1016/j.medengphy.2025.104400]

Availability:
This version is available at: 11583/3002457 since: 2025-08-18T15:48:26Z

Publisher:
Elsevier

Published
DOI:10.1016/j.medengphy.2025.104400

Terms of use:

This article is made available under terms and conditions as specified in the corresponding bibliographic description in the repository

Publisher copyright

(Article begins on next page)

19 November 2026

Medical Engineering and Physics 143 (2025) 104400



Contents lists available at ScienceDirect

Medical Engineering and Physics

journal homepage: www.elsevier.com/locate/medengphy



Paper



A cascade approach for the early detection and localization of myocardial infarction in 2D-echocardiography

Carolina Gomez [a], Annalisa Letizia [a], Vincenza Tufano [a], Filippo Molinari [b], Massimo Salvi [b,*]

[a] Teoresi Group S.p.a., Via Perugia, 24, 10152 Turin, Italy
[b] Biolab, PoliTo[BIO]Med Lab, Department of Electronics and Telecommunications, Politecnico di Torino, Corso Duca degli Abruzzi 24, 10129 Turin, Italy

ARTICLE INFO

Keywords:
Artificial intelligence
2D-Echocardiography
Left ventricle segmentation
Myocardial infarction
Deep learning
Cascade approach

ABSTRACT

Myocardial infarction (MI) detection and localization through echocardiography are crucial for effective patient management. However, current diagnostic approaches rely heavily on visual assessment, which can be subjective. In this work we developed a cascade framework for automated MI diagnosis and localization in echocardiograms. Our method combines deep learning for left ventricle wall segmentation with machine learning classification using clinically relevant features. Specifically, we employ a U-Net architecture for segmentation, followed by a two-stage Random Forest classifier for MI detection and localization. We trained and evaluated our approach on two public datasets – CAMUS and HMC-QU. The proposed method achieved 100 % sensitivity and 89.8 % specificity for segment identification, outperforming single-stage classification methods. To the best of our knowledge, this is the first study to apply a multi-step artificial intelligence system combining segmentation and classification for MI diagnosis from echocardiography. This interpretable cascade framework exhibits high performance for early detection and localization of myocardial infarction, demonstrating potential as a clinical decision support tool.

1. Introduction

Myocardial infarction (MI) is caused by prolonged ischemia resulting from coronary artery disease (CAD) [1]. CAD is the most diagnosed heart disease and the leading cause of death worldwide [2]. Early detection and localization of MI are critical to prevent wall ruptures, arrhythmias, heart failure, and sudden cardiac death [3,4]. Identification of the affected segment can guide treatment decisions, including the selection of appropriate medications or interventions. Locating the affected segment can also aid in monitoring the disease's progression and evaluating the treatment effectiveness. Therefore, accurately locating the affected segment is crucial for effectively managing MI.

In patients affected by MI, the contractile function of the affected area decreases due to cell injury, inflammation, and fibrotic tissue replacement [3]. Reduced wall motion is the first abnormality to occur after the onset of myocardial ischemia, preceding metabolic and electrocardiographic abnormalities [4]. Medical imaging, particularly 2D echocardiography, is a non-invasive, cost-effective and simple procedure used to diagnose heart diseases [5]. Multiple studies have demonstrated that motion visualization of the heart is an effective and early-stage technique to detect MI, limit the extent of damage and prevent complications [6,7].

The motion of the left ventricular (LV) wall is of particular interest in detecting MI. Regional wall motion abnormalities (RWMA) are currently evaluated by cardiologists, a process that can be subjective and operator dependent. To address this issue, speckle tracking echocardiography (STE) has been developed. STE assists cardiologists by using computer vision to track the displacement of "speckle patterns" of the myocardium in 2D echocardiography, assessing deformation and strain during the cardiac cycle [8]. Although STE reduces the subjectivity of visual estimation and diagnosis, some limitations remain, such as sensitivity to frame rate and image quality, and the lack of standardization due to differences in algorithms between vendors [9,10]. Nonetheless, many studies using the speckle tracking technique achieve a sensitivity of around 80 % to 85 % in identifying infarcted segments [11,12].

Deep learning (DL) and quantitative approaches are becoming more prevalent in ultrasound imaging due to the increased data availability [13–15]. Convolutional Neural Networks (CNNs) with U-Net

* Corresponding author at: Politecnico di Torino, Corso Duca degli Abruzzi 24, 10129 Torino, Italy.
E-mail address: massimo.salvi@polito.it (M. Salvi).

https://doi.org/10.1016/j.medengphy.2025.104400
Received 7 November 2024; Received in revised form 3 March 2025; Accepted 16 July 2025
Available online 17 July 2025
1350-4533/© 2025 The Authors. Published by Elsevier Ltd on behalf of IPEM. This is an open access article under the CC BY license (http://creativecommons.org/licenses/by/4.0/).

architectures are commonly used for segmentation tasks. For example, Leclerc et al. [16] designed a CNN to segment echocardiographic images from 500 patients, achieving automatic masks in 0.14 s per image with a Dice score of 0.939. More recently, Degerli et al. [17] tested a different CNN model on an echocardiography dataset from 109 patients for left LV wall segmentation, achieving 95.72 % sensitivity and 99.6 % specificity with low processing times.

However, few studies have focused on MI classification from ultrasound images, primarily due to the lack of publicly available datasets. The HMC-QU dataset [11], released in 2020, is the first publicly available echocardiographic dataset for MI detection. The results from these studies are summarized in Table 1. Initial approaches focused on simpler techniques, such as fixed thresholds on LVEF and maximum segment displacement [11], which provided a foundation for MI detection but achieved limited performance (sensitivity: 85.97 %, specificity: 70.10 %). More recent studies have progressively moved towards machine learning techniques [17] and ensemble learning methods [18], which have demonstrated significantly improved performance with sensitivities exceeding 94 %.

Several studies have demonstrated that the extent of RWMA in MI patients can vary significantly due to differences in metabolic characteristics and ischemic tolerance of the affected myocardium [20]. As a result, binary threshold approaches for detecting MI may be limited and may not align with clinical parameters used in echocardiography evaluation [21]. To improve clinical diagnosis, additional parameters should be included in the classification process, particularly for identifying ischemia. Although left ventricle ejection fraction (LVEF) is commonly used, it alone is insufficient as its value varies among patients [22,23]. Global longitudinal strain (GLS) is an additional parameter that considers physiological characteristics and provides more information for identifying ischemia. However, GLS alone cannot be used for classification via a threshold approach, as there is no consensus on the appropriate cutoff value [24].

This study aims to develop an automatic algorithm for MI detection and localization in ultrasound images. This algorithm employs deep learning for LV segmentation and machine learning for classification, aiming to create a diagnostic tool that incorporates clinically relevant information for cardiologists. The main contributions of this paper can be summarized as follows:

- A novel cascade approach that localizes myocardial segments affected by local ischemia, enabling more targeted diagnosis and treatment.
- Combination of two distinct datasets to train the deep neural network for LV segmentation, resulting in improved generalization and segmentation accuracy.
- Integration of clinical parameters like GLS and LVEF as training features for MI identification, resulting in improved sensitivity and specificity of the model.
- Incorporation of AI explainability and visual model validation in the decision-making process. This enables cardiologists to interpret the results, improving transparency and reliability of our approach.

Table 1
Current published works for MI detection approaches with HMC-QU dataset.

Author	Method	# Patients	Computational time	Performance
Kiranyaz et al., 2020 [11]	Fixed threshold on LVEF and maximum segment displacement	160 (A4C view)	36.9 s/cardiac cycle	Sensitivity: 85.97 %; Specificity: 70.10 %
Degerli et al., 2021 [17]	ML techniques with arear and displacement features	109 (A4C view)	2.58 s/cardiac cycle	Sensitivity: 89.01 %; Specificity: 75.36 %
Hamila et al., 2022 [19]	CNN-based pipeline for LV segmentation and MI detection	162 (A4C view)	0.44 s/cardiac cycle	Sensitivity: 95 %
Nguyen et al., 2023 [18]	Ensemble learning of features from multiple LV segmentation models	109 (A4C view)	–	Sensitivity: 94.1 %; Specificity: 88.3 %
Degerli et al., 2024 [4]	ML techniques with maximum displacement feature	130 (both A4C and A2C views for each)	59.15 s/cardiac cycle (multi-view echocardiography)	Sensitivity: 86.25 %; Specificity: 84.00 %

ML: Machine learning; CNN: Convolutional Neural Networks.

2. Materials and methods

The proposed methodology involves three main steps: (i) LV wall segmentation, (ii) Feature extraction, and (iii) MI detection and localization, as illustrated in Fig. 1. This section provides an overview of the datasets used and the data division for the project. Each step will then be explained in detail.

2.1. Datasets

This study utilized two publicly available datasets of echocardiographic exams. The first dataset is the Cardiac Acquisitions for Multi-structure Ultrasound Segmentation (CAMUS) dataset, which contains echocardiographic exams from 500 patients, including manual annotations for the left ventricle endocardium, myocardium, and left atrium [16]. The dataset includes patient information such as gender, age, image quality, LV volume, and LVEF. After excluding exams with incomplete annotations or wall segments, 182 patients remained in the study.

The second dataset was created in collaboration between Hamad Medical Corporation Heart Hospital, Qatar University, and Tampere University (HMC-QU) and consists of 162 recordings of apical four-chamber views from 93 MI and 69 non-MI patients [4]. Ground-truth labels are provided for six left ventricle wall segments. The dataset also includes 109 recordings with a ground-truth segmentation mask for the whole LV wall for each frame in one cardiac cycle. Of these, 109 recordings include complete left ventricle segmentations (both endocardial and epicardial boundaries). However, manual review revealed defects in some segmentations (e.g., bifurcated endpoints), resulting in only 97 high-quality recordings being used to train the deep network. For the MI classification task, we used 148 recordings after excluding 14 that did not meet our quality criteria. These exclusions were based on specific factors such as incomplete cardiac cycles, significant artifacts, or poor image quality, which could affect the reliability of MI classification.

Data division for the segmentation and classification tasks is presented in Table 2. No institutional review board approval was required as only de-identified public datasets were used.

2.2. Preprocessing and LV wall segmentation

To ensure consistency and enhance the area of interest, we performed preprocessing on the two datasets used in our study. The aim was to obtain a homogeneous pool of data. For the HMC-QU dataset, we: (i) automatically extracted individual frames from all the registrations; (ii) converted the frames to grayscale; and (iii) cropped images to closely resemble the images from the CAMUS dataset. We then applied an automatic equalization technique [25] to enhance the visibility of the myocardium in all images. This technique effectively increases the contrast in images that have a narrow range of intensity values, as shown in Fig. 2.

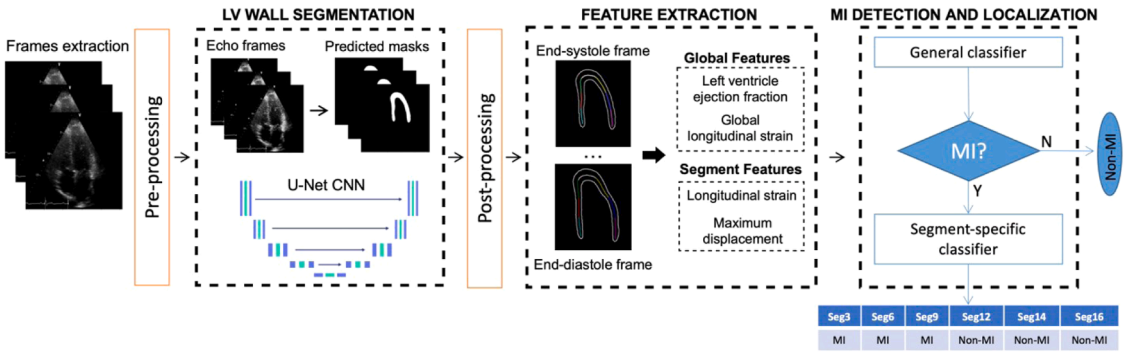


Fig. 1. Schematic representation of the proposed algorithm for MI detection and localization. The algorithm comprises three steps: (1) LV wall segmentation using a U-Net model, (2) feature extraction using a combination of clinical parameters, and (3) MI detection and localization using a two-stage classifier. The general classifier performs a patient-level classification, and only positive patients proceed to the segment-specific classifier for MI localization within the LV wall.

Table 2
Patient division for segmentation and classification tasks. A deep learning model was used to identify LV wall segments, with the number of frames indicated in parentheses. Meanwhile, a machine learning-based model was employed for MI classification, with brackets indicating the number of wall segments.

Task	Technique	Dataset	Train	Val	Test
LV wall segmentation	Deep learning	CAMUS	127 (253)	19 (37)	36 (72)
		HMC-QU	69 (1424)	10 (203)	18 (407)
MI classification	Machine learning	HMC-QU	118 (710)	–	30 (178)

To segment the LV wall from echocardiogram images, we used a deep learning approach. This choice was motivated by the availability of data and need for efficient inference. Specifically, we implemented a fully convolutional neural network (CNN) based on the U-Net architecture (Fig. 3). To optimize our segmentation model, we conducted a comprehensive evaluation of several common backbone architectures for the U-Net. This evaluation included MobileNetV2, ResNet18, ResNet50, DenseNet121, and EfficientNet-B4. During the optimization process, we assessed each architecture based on various performance metrics, including Dice score, sensitivity, specificity, and inference time. After this analysis, we selected EfficientNet-B4 as our backbone architecture. This choice was motivated by its superior performance in balancing segmentation accuracy with inference speed. Further details on the optimization process can be found in the Supplementary Materials.

We trained the entire network (both encoder and decoder paths) from scratch, without employing transfer learning. All images were resized to 512 × 512 to match the network's input size. Additionally, we performed data augmentation on input images using the TensorFlow library, rotating images up to 10 degrees and zooming up to 10 %. We used the Jaccard loss function with a batch size of 4 and trained for a maximum of 20 epochs. We also implemented early stopping based on the validation IoU score and used the Adam optimizer. Training was performed on a workstation with an NVIDIA RTX Quadro A600 GPU.

The CNN automatically generates precise LV wall segmentations from echocardiogram video frames. Inference takes approximately 50 ms per frame, allowing segmentation of a sample echocardiogram video

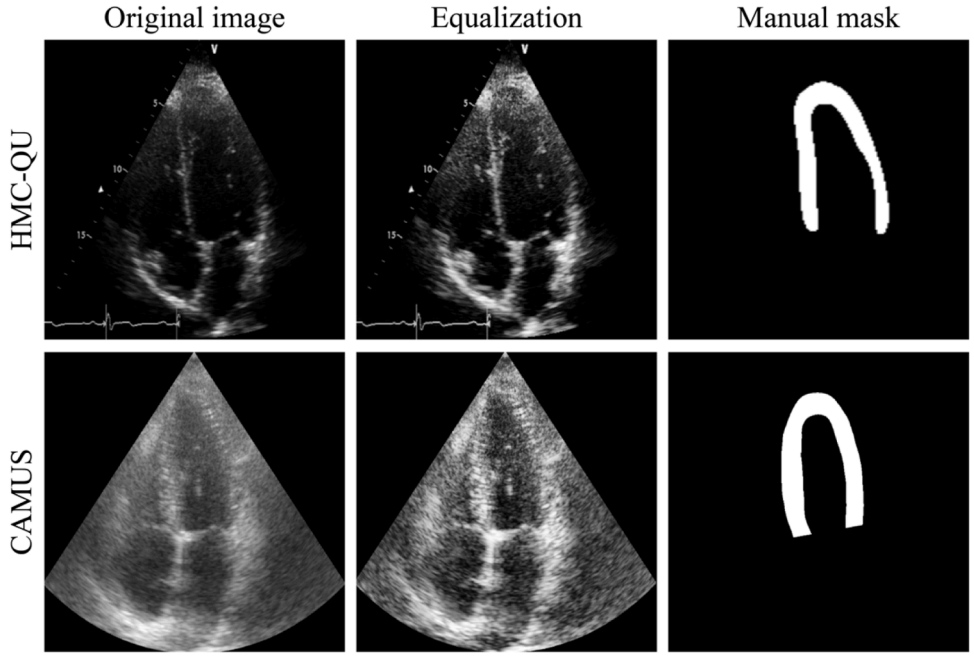


Fig. 2. Sample frame of HMC-QU and CAMUS datasets before and after image equalization. LV wall manual mask is included for reference. Note that the HMC-QU masks appear to have a different resolution due to the varying spatial resolution of the original echocardiography recordings (ranging from 422 × 636 to 768 × 1024 pixels).

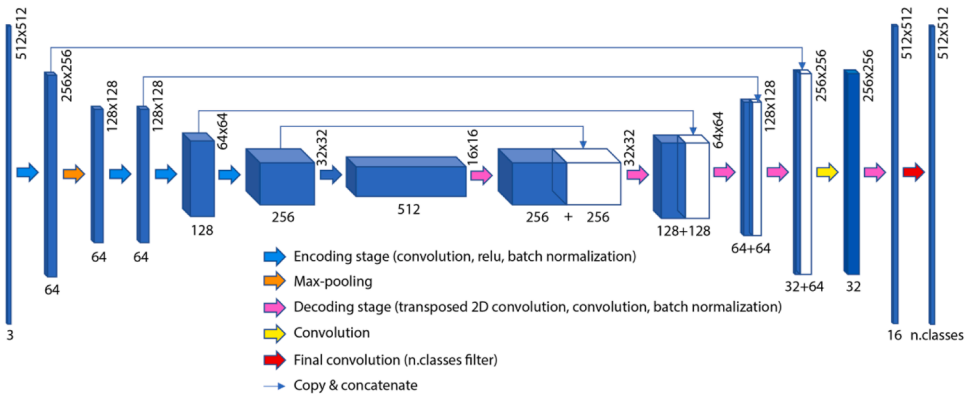


Fig. 3. Architecture of the deep network employed to perform LV segmentation. A U-Net with EfficientNet B4 backbone was implemented using Keras framework.

in about 2 s total.

2.3. Post-processing and segment division

Post-processing was implemented to address potential issues from the CNN segmentation. We applied a morphological closing operation using a 10 × 10 pixel structural element, facilitating spatially contiguous and complete LV segmentations in each frame. This process also mitigated fragmentation or incomplete boundaries that could result from the model alone. Next, the myocardium layer was extracted as the middle lining of the LV wall mask using the skeletonization algorithm proposed by Lee et al. [26]. The left ventricle wall was then divided according to the standardized 17-segment model established by the American Heart Association (AHA) and described by Cerqueira et al. [27]. However, as our study used single-plane echocardiographic images, we adopted a simplified sequential numbering approach for segmenting (Fig. 4b). While this does not exactly match the 17-segment classification, it allowed us to uniquely assess each myocardial segment visible in the single-plane view, facilitating the entire analysis. The sequential numbering represented each segment with a single number from base to apex. Fig. 4 also illustrates the correspondence between the standard 17-segment American Heart Association (A4C) numbering system and our adopted sequential numbering method. Although less standardized, the sequential approach was necessary given the single-plane image format.

In the HMC-QU dataset, only the six moving segments were provided

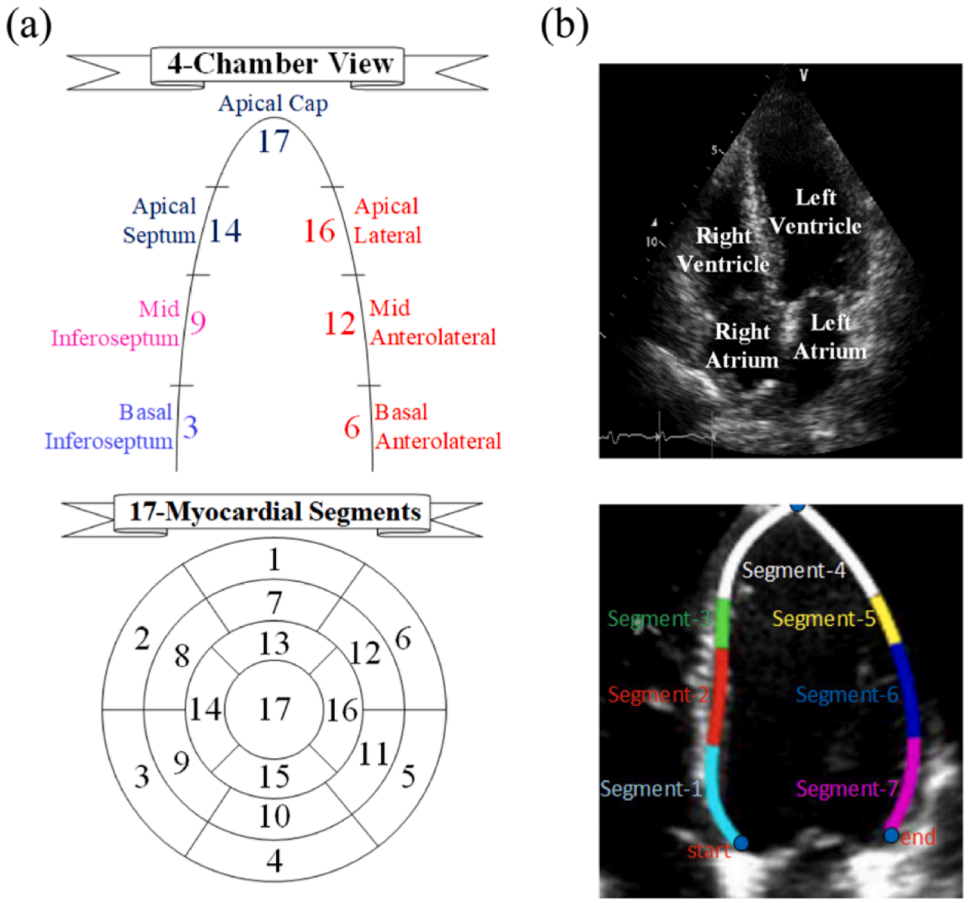


Fig. 4. (a) 17-segment model established by the American Heart Association (AHA). (b) In-vivo images and sequential numbering of segments in the four-chamber view.

with classification labels. This is because, in the apical four-chamber view, the topmost segment representing the apical cap does not exhibit inward motion [28]. Therefore, in this study, although the segmentation adheres to the 17-segment model, the apical cap was excluded from subsequent calculations. The LV wall segmentation (including both endocardial and epicardial boundaries) was used as input for the partitioning process. To divide the segmented myocardium, we used the midpoint between its left and right portions. Subsequently, we assigned each of the six segments of interest 2/7 of the length of its corresponding portion, while the apical cap occupied the remaining 1/7 on each side (Fig. 4). This partitioning scheme enabled consistent extraction and division of the LV myocardium into segments, which was crucial for the subsequent stages of our methodology.

2.4. Features extraction

For training and testing the ML models, global and segment features were extracted from the mask and segment divisions obtained from the myocardial wall tracing. This study utilizes features corresponding to clinical parameters commonly used in echocardiography evaluation. The goal is to provide cardiologists with interpretable values and train the classifiers using physiological information.

In terms of global assessment, the selected features were left ventricular ejection fraction (LVEF) and global longitudinal strain (GLS). For segment assessment, longitudinal strain (LS) and segment displacement were employed. All features were obtained from the end-systolic and end-diastolic frames within each cardiac cycle. These frames were automatically identified from the endocardial segmentation masks, with the end-diastolic frame corresponding to the maximum left ventricular cavity area and occurring first in the sequence, followed by the end-systolic frame with minimum area. To facilitate direct comparison between different patients and eliminate the effects of variability in echo exams, all features were normalized with respect to end-diastolic measurements. This normalization ensures the ability to make meaningful comparisons and mitigates the impact of dimension variability.

Since this study employs a single 2D echocardiogram view, volumetric calculation of the LVEF was not possible. Instead, to estimate LVEF from the segmentation results, several area-based formulas were evaluated against true reference LVEF values in the CAMUS dataset. Following Kiranyaz et al. [11], this study approximates the volumetric fraction using the area fraction (Eq. (1)):

$$LVEF \approx 1 - \left(\frac{A_{ES}}{A_{ED}}\right)^{3/2} \tag{1}$$

where A_{ED} and A_{ES} indicate the area, in number of pixels, inside the LV cavity at end systole and end diastole, respectively. The formula shown in Eq. (1), which uses a 3/2 power relationship between end-systolic and end-diastolic areas, demonstrated the lowest errors. Specifically, it produced the minimum mean absolute error and mean relative error compared to alternatives like the one proposed by Kiranyaz et al. [11].

Strain parameters have shown greater sensitivity than LVEF in assessing early myocardial dysfunction and detecting abnormal contraction patterns, even when LVEF appears normal [29,11]. GLS measures the fractional length change between systole and diastole, providing valuable information on myocardial contractility (Eq. (2)):

$$GLS = \frac{L_{ES} - L_{ED}}{L_{ED}} = \frac{L_{ES}}{L_{ED}} - 1 \tag{2}$$

where L_{ED} and L_{ES} indicate the LV length, measured from mid-base to apex, at end diastole and end systole, respectively. This feature can also be extended to study regional myocardial function by evaluating the strain of each individual segment. In this case, the length change corresponds to that of each segment.

RWMA are directly associated with the presence of MI and the subsequent scarring and replacement of myocardial tissue with fibrotic tissue. To measure wall motion, a displacement feature is incorporated within our classifier. To facilitate comparison with previous models and results, a normalized maximum displacement value is calculated for each of the six segments of interest, following the approach described by Kiranyaz et al. [11]. The displacement feature is obtained by determining the average displacement between systole and diastole frames (maximum displacement) at five equidistant points within each segment. This value is then normalized by dividing it by the minimum distance between opposing segments. Normalizing the displacement feature ensures that the measurements are standardized and allows for easier model and result comparisons in subsequent analyses. Fig. 5 shows the feature extraction process from the LV segmentation.

2.5. Classification and cascade approach

The Random Forest algorithm was selected after a comprehensive comparison with other machine learning techniques, including Support Vector Machines (SVM) and K-Nearest Neighbors (KNN). Detailed results of this comparative analysis, including hyperparameter tuning and performance metrics for each method, are provided in the Supplementary Information.

The architecture of the RF is optimized using grid search. Key hyperparameters tuned include the number of trees (20–50), maximum tree depth (5–30), minimum samples for node splitting (2–10) and leaf nodes (1–5). The model is optimized based on accuracy to balance sensitivity and specificity. The final RF model consists of 50 decision trees, each trained on bootstrap samples of the data. Feature bagging is employed, considering a number of features equal to the square root of the total number of features for each split. Initially, we train a model on the concatenation of all features, which includes 14 features in total: two global features and two segment-specific features for each of the six segments. This model determines whether the patient presented MI or not. If the patient is classified as having MI, we propose a cascade approach to identify the specific segments involved in the infarction. To achieve this, we train six different classifiers, each specific to one of the segments. For each model, four features are provided as input: the two global features and the two features specific to the segment of interest.

Prior to training the models, we apply data augmentation techniques to enhance the representation of pathological cases. Through this process, we generate a total of 15 additional synthetic patients (corresponding to 90 segments) with MI characteristics, supplementing our base dataset of 148 real patients from HMC-QU. The synthetic data generation is based on statistical features calculated from 10 real patients in the HMC-QU dataset who had all six segments labeled as infarcted. Specifically, we extract the average, minimum, maximum, and standard deviation for each cardiac motion parameter. These statistical values, combined with abnormal ranges reported in the literature, are used to synthetically generate new patients. These augmented patients are included only in the training set to enhance the learning of pathological patterns while maintaining evaluation on real clinical data.

2.6. Performance metrics

In the context of MI detection, we place particular importance on avoiding false negatives, as missing a true positive could have severe clinical consequences. Therefore, sensitivity is considered a more significant metric than specificity in this evaluation. To account for the potential imbalance between these metrics, we also evaluate the machine learning models for classification using the area under the receiver operating characteristic (ROC) curve (AUC). The AUC provides a comprehensive assessment of the model's performance across different thresholds, helping us gauge its overall discriminative ability.

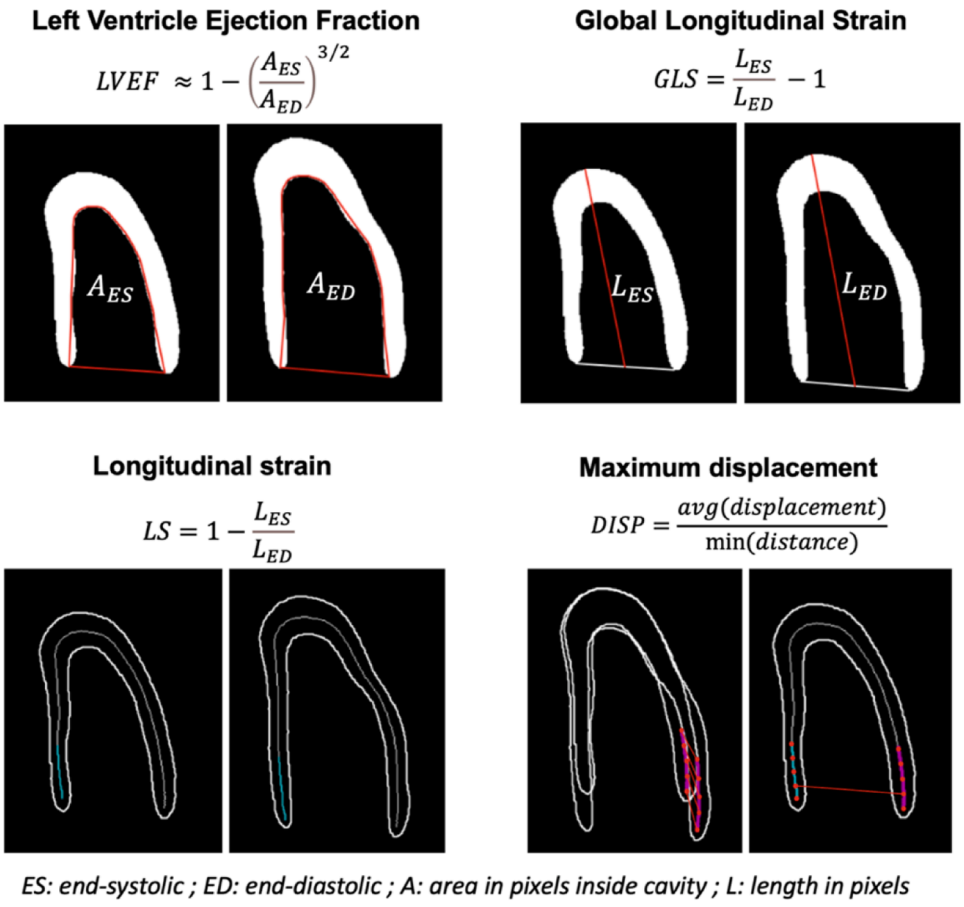


Fig. 5. Visual representation of the calculation of clinically relevant features. LVEF: left ventricle ejection fraction, GLS: global longitudinal strain, LS: longitudinal strain, DISP: segment maximum displacement.

3. Results

3.1. Segmentation of the left ventricular wall

Table 3 summarizes the performance of the U-Net for the segmentation of the LV wall. The quantitative metrics demonstrate the accuracy of the network in identifying the LV, with comparable segmentation performance seen across all subsets, suggesting no overfitting issues. The errors presented for the LV ejection fraction (LVEF) calculation correspond to the CAMUS dataset, which provided real LVEF information. As shown in Table 3, the errors are comparable across all three subsets, with values around 10 %.

3.2. Classification of MI patients

In this study, we developed two different classification approaches using the RF algorithm: a general patient classifier and a segment-specific classifier comprising six individual models, one for each myocardial segment. Table 4 reports the performance of the segment-specific classifiers. As shown in the table, the sensitivity of individual classifiers ranges from 88.9 % to 100 %, while specificity ranges from 75.9 % to 95 %. Notably, classifiers trained on the two segments near the apical part of the ventricle (segments 3 and 5) achieve a sensitivity of 100 %, while classifiers trained on segments in the basal region (segments 1 and 7) obtain high specificities.

In our cascade approach, we applied the segment-specific classifiers only to patients initially classified as having MI by the general patient classifier. Table 5 shows the performance of the general classifier and the cascade approach. Our proposed cascade approach achieved the highest performance across all metrics evaluated. The 100 % sensitivity indicates that all true MI segments were correctly identified within the subset of patients pre-classified MI-positive. This cascade approach served two important purposes:

1. It validated the initial classifications of patients as having MI by the general classifier, confirming the accuracy of those predictions.

Table 3
Segmentation performance of the LV wall using the U-Net model on train (196 patients), validation (29 patients), and test (54 patients) subsets. The average absolute error in the LVEF calculation for the CAMUS dataset is also reported.

Subset	Segmentation metrics (CAMUS, HMC-QU)			LVEF calculation (CAMUS)
	Dice	Sensitivity	Specificity	Mean absolute error
Training	96.3 %	96.9 %	99.8 %	9.90 %
Validation	94.4 %	95.0 %	99.6 %	7.32 %
Test	96.0 %	96.5 %	99.8 %	11.6 %

Table 4
Quantitative metrics on the test set (45 patients) for the segment-specific classification using RF.

Segment	TP	FN	TN	FP	Accuracy	Sensitivity	Specificity
Seg 1	8	1	32	4	88.9 %	88.9 %	88.9 %
Seg 2	15	1	22	7	82.2 %	93.8 %	75.9 %
Seg 3	22	0	20	3	93.3 %	100 %	87 %
Seg 5	16	0	25	4	91.1 %	100 %	86.2 %
Seg 6	8	1	33	3	91.1 %	88.9 %	91.7 %
Seg 7	5	0	38	2	95.6 %	100 %	95 %
Average					90.4 %	95.3 %	87.5 %

Table 5
Results of the classification models based on RF for MI classification in the test set (45 patients). For the segment-specific classification model, the average performance among all the segments is reported.

Model	Accuracy	Sensitivity (MI)	Specificity (Non-MI)
General classification	91.1 %	96.3 %	83.3 %
Segment-specific classification (alone)	90.4 %	95.3 %	87.5 %
Cascade approach (proposed)	94.9 %	100 %	89.8 %

2. It provided a more detailed diagnosis by enabling identification of the specific myocardial region(s) presenting infarction. This would allow for targeted and precise treatment planning.

We also evaluated the performance of the general classifier and each segment specific classifier separately using ROC curves and AUC calculations. In addition, we compared a fixed threshold method to evaluate the feasibility of a simpler approach compared to machine learning. However, we found that different threshold values were needed for each model, indicating that a fixed threshold is not suitable for this classification task. The RF classifier consistently achieved the highest AUC for all models, indicating its superiority as a classification strategy (Fig. 6).

3.3. Comparison with state-to-the-art studies on HMC-QU dataset

To evaluate the effectiveness of our proposed approach, we compared its performance with state-of-the-art methods for MI detection using the HMC-QU dataset. Table 6 presents the comparison of our method against three notable approaches from recent literature. The comparison metrics include overall accuracy, sensitivity for MI detection, and specificity for non-MI cases.

Our cascade approach demonstrates superior performance across all metrics. Notably, it achieves an accuracy of 94.90 %, significantly outperforming the next best method by Nguyen et al. [18], which reported an accuracy of 91.40 %. The specificity of 89.80 % achieved by our method for non-MI cases also surpasses previous methods, demonstrating a well-balanced performance in distinguishing between MI and non-MI cases. It's worth noting that our approach not only achieves better performance metrics but also provides additional clinical value through segment-specific localization. While previous methods like Nguyen et al.'s ensemble learning approach showed promising results (94.1 % sensitivity, 88.3 % specificity), they focused solely on binary MI classification without segment localization.

3.4. Features importance and explainability of the results

This study assessed the importance of features individually for the general patient classifier and for each of the segment-specific classifiers. The SHAP (Shapley Additive Explanations) python package was used to determine the relevance of each feature by calculating its SHAP values [30]. These values measure the individual contribution of each feature to the final prediction. To quantify the SHAP feature importance, we analyzed the mean absolute SHAP value for each feature across all patients. For the general classifier, LVEF had the highest mean SHAP value at 0.046, followed by segment displacement. This confirms that LVEF made the largest average contribution to classifications by the general model. The consistency of LVEF as one of the top two most influential features across all models underscores its clinical significance in MI diagnosis [31].

When examining the segment classifiers individually, we found variations in most important features for different segments. For basal segments, such as 1 and 7, classifier relied most heavily on displacement (mean SHAP of 0.032 and 0.05, respectively). Other notable findings include GLS and longitudinal strain emerging as highly ranked factors for apical segments, such as segment 3 (mean SHAP 0.037). This aligns with prior evidence of strain parameters being more sensitive markers of dysfunction in these regions [32]. This analysis also confirmed the importance of training separate classifiers for each segment, as the order of feature importance varied among the different classifiers.

Fig. 7 presents a beeswarm plot illustrating the importance of features, where higher positions indicate greater significance. Each dot

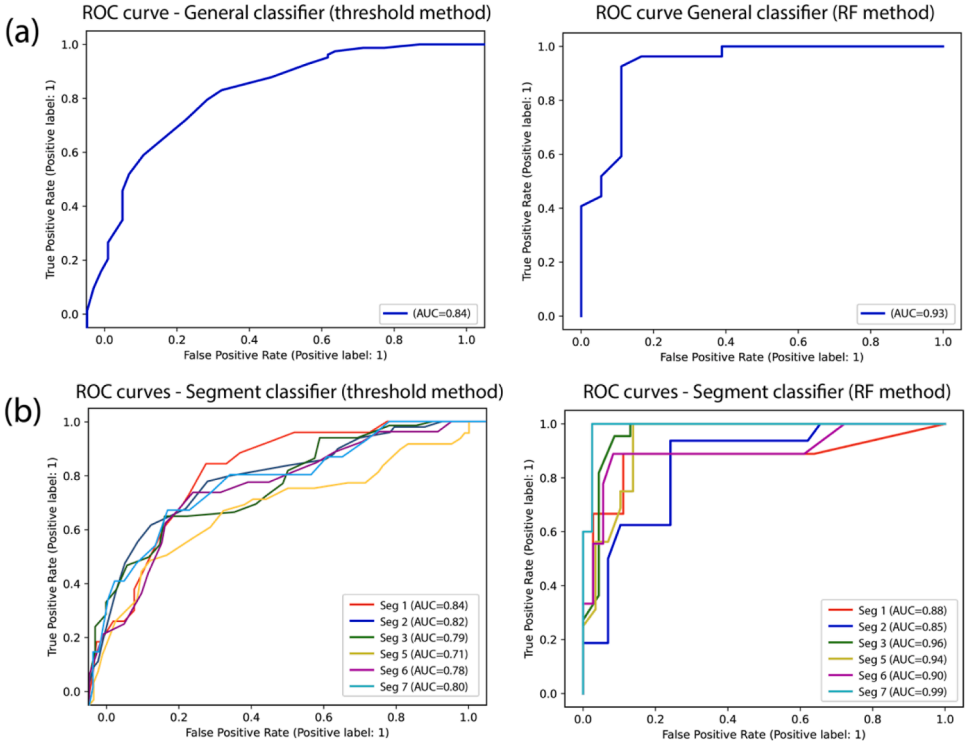


Fig. 6. Comparison of the ROC curves between a threshold method and the proposed RF method. (a) General classifier, (b) segment-specific classifier.

Table 6
Comparison for MI detection approaches with HMC-QU dataset.

Work	#Patients	Method	Accuracy	Sensitivity (MI)	Specificity (Non-MI)
Kiranyaz et al., 2020 [11]	160	SVM	80.24 %	85.97 %	70.10 %
Degerli et al., 2021 [17]	109	Active Polynomials	83.13 %	89.01 %	75.36 %
Hamila et al., 2022 [19]	162	CNN	–	95 %	–
Nguyen et al., 2023 [18]	109	Ensemble learning	91.40 %	94.1 %	88.3 %
Degerli et al., 2024 [4]	130	RF	85.38 %	86.25 %	84.00 %
Proposed cascade approach	148	RF	94.90 %	100 %	89.80 %

SVM: Support Vector Machine; CNN: Convolutional Neural Networks; RF: Random Forest.

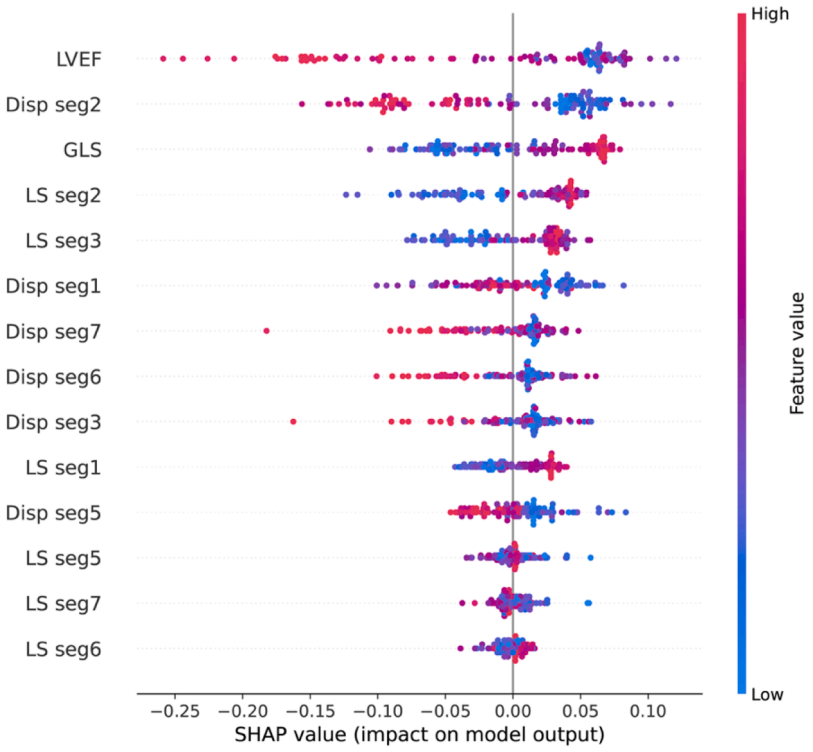


Fig. 7. Beeswarm plot of the classification model. LVEF: left ventricle ejection fraction; Disp: segment maximum displacement; GLS: global longitudinal strain; LS: segment longitudinal strain.

represents a single patient, and the color represents the feature value relative to other samples. Positive SHAP values indicate that the feature value contributes to a positive classification (MI), while negative SHAP values denote a contribution to a negative classification (Non-MI). The plots clearly show that low LVEF values are concentrated on the right side, consistently leading to an MI classification. Interestingly, some high LVEF values are also present in the right part of the graph, indicating that MI patients can have high LVEF values. This finding highlights the importance of considering feature combinations for accurate classification, as no single feature alone can determine the final classification.

To better understand the factors contributing to misclassifications, we conducted a detailed analysis of misclassified patients. The analysis revealed that misclassifications frequently occurred when:

1. Non-MI patients exhibited lower LVEF values typically associated with MI.
2. MI patients presented higher LVEF values not usually indicative of infarction.

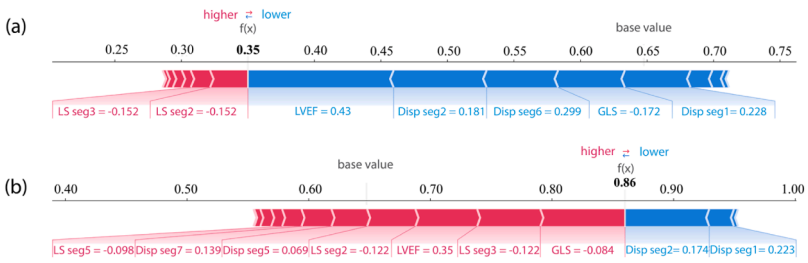


Fig. 8. Force plots illustrating feature values, their contributions to classification, and predicted probability of belonging to the MI class for two misclassified patients in the test set. (a) false negative patient, (b) false positive patient.

Additionally, segment displacement played a role, as lower values - more common in Non-MI cases - could lead to incorrect MI predictions. Fig. 8 illustrates these trends visually, displaying force plots of feature values, their impact on classification, and predicted MI probability for two misclassified patients. One plot depicts a false negative where strong evidence pointed to MI, but the model predicted otherwise. The other shows a false positive where features aligned more closely with a Non-MI profile. This in-depth interpretability analysis provided valuable insights into how specifics features can influence misclassifications. This analysis also improved model transparency by identifying scenarios where predictions diverged from expected outcomes. Overall, this examination enhanced our understanding of classification behaviors and limitations.

4. Discussion

Our proposed method for myocardial infarction detection offers several key advantages, including a novel cascade approach that enables the localization of the myocardial segment affected by ischemia. Our approach involves a global and local classification process. This cascade approach provides greater accuracy and specificity in identifying the specific area affected by MI, making it a valuable tool for cardiologists in the diagnosis and treatment of patients. The proposed framework is also fast, taking an average computational time of 28.4 s to process a 41-frame echocardiography video.

To the best of our knowledge, this is the first work to employ a multicenter data to train a deep neural network for LV segmentation. This study uniquely uses real clinical parameters of cardiac function for classification. Global and segmental physiological parameters are extracted, which can serve as a validation tool for the cardiologist. The proposed cascade approach offers a double verification when the algorithm detects MI. Additionally, by classifying the individual segments, a more informative diagnosis is obtained. To enhance model interpretability, we integrated AI explainability methods and visual validation tools to support result interpretation. This feature enables cardiologists to better understand and validate each step of the process, empowering them to make more accurate diagnoses and confident treatment decisions.

Unlike previous studies [11,16,17], we implemented quality control checks on the dataset used. Specifically, we excluded patients with incomplete annotations from the CAMUS dataset, and segmentations containing defects from the HMC-QU dataset. This approach ensured that only recordings with reliable ground truths were used for training and testing our method.

Our cascade approach for MI detection and localization demonstrates significant improvements over existing methods. Previous studies using the HMC-QU dataset reported lower performance metrics. For instance, Kiranyaz et al. [11] achieved 85.97 % sensitivity and 70.10 % specificity using a fixed threshold approach, while Degerli et al. [4] reported 86.25 % sensitivity and 84.00 % specificity. In contrast, our two-stage Random Forest classifier achieved 100 % sensitivity and 89.8 % specificity for segment identification, surpassing the performance of these single-stage classification methods. The high sensitivity of our approach is particularly crucial for early MI detection, potentially enabling timely interventions on patient. Furthermore, the specificity of 89.8 % represents a substantial improvement over previous methods, reducing false positives and potentially minimizing unnecessary interventions or further testing.

While our approach achieved great performance metrics (almost 90 % specificity and 100 % sensitivity), it is important to note that our main goal was not to get the best accuracy. Rather, we focused on creating an understandable method that makes use of clinically important information. By using clinical characteristics in the decision-making process, this design aims to increase physicians' trust in the AI system. The model not only makes predictions but also highlights which clinical features contributed most to each classification, making it a more practical and trustworthy tool for clinical implementation.

The main limitation of the study is that the proposed segmentation network only works with A4C view echocardiography, which limits the acquisition features to this view. Consequently, LVEF cannot be calculated as volumetric measure but can only be estimated using an approximation formula (Eq. (1)). Given the high relevance of this feature, future studies should focus on improving its approximation. Additionally, our strict data curation approach, while necessary to ensure reliable training data, creates potential limitations for generalizability. The trade-off between data quality and quantity particularly affects our results, as we excluded cases with incomplete annotations or segmentation defects. Moreover, the evaluation has been conducted on a specific dataset (HMC-QU), and further validation on independent data is necessary to assess the generalizability of our approach. Future work should focus on making the approach more robust to imperfect data, potentially through semi-supervised learning techniques that could leverage both labeled and unlabeled data [33]. Another limitation of our current study is the lack of direct comparison between our model's performance and that of experienced radiologists. Future work should include an evaluation where both our AI model and a panel of experienced radiologists independently analyze the same set of echocardiograms. This would allow for a direct comparison of sensitivity, specificity, and accuracy in MI detection and localization. Additionally, it would be beneficial to assess the time efficiency of our model compared to manual analysis by radiologists.

While our cascade approach aims to balance accuracy and computational efficiency, we acknowledge that alternative strategies, such as feature fusion across segments, could potentially enhance overall performance. Future work could explore combining the most discriminative features from each segment into a unified classifier, which might improve accuracy while still providing segment-specific insights. In terms of future development, it is also important to consider incorporating uncertainty quantification [34] for the classifiers. By quantifying the uncertainty associated with the classification results, we can provide additional information to the cardiologists regarding the confidence and reliability of the predictions made by the models.

5. Conclusion

The proposed cascade approach presents a highly effective algorithm for the early detection and localization of myocardial infarction in 2D-echocardiography. By employing a systematic and progressive methodology, the algorithm outperforms the general classifier, achieving a remarkable sensitivity of 100 % and a specificity of 89.8 %. The significant improvement in classification performance highlights the potential of the cascade approach as a valuable second-opinion tool for early diagnosis of myocardial infarction. Beyond diagnostic performance improvements, this AI-assisted approach holds promise to aid clinical decision-making. Precisely identifying the infarcted segment could guide targeted treatment, such as revascularization of the appropriate coronary artery. It may also influence medication selection by indicating specific areas of reduced contractility.

Ethical approval

Not required.

Funding

No funding for this research.

CRediT authorship contribution statement

Carolina Gomez: Methodology, Software, Validation, Data curation, Writing – original draft. **Annalisa Letizia:** Conceptualization, Validation, Writing – review & editing. **Vincenza Tufano:** Conceptualization,

Validation, Writing – review & editing. **Filippo Molinari:** Supervision, Writing – review & editing. **Massimo Salvi:** Methodology, Supervision, Writing – original draft.

Conflict of interest

The authors declare no conflict of interest.

Supplementary materials

Supplementary material associated with this article can be found, in the online version, at doi:10.1016/j.medengphy.2025.104400.

References

[1] Shen Y-T, Chen L, Testani JM, Regan CP, Shannon RP. Animal models for cardiovascular research. Animal Models for the Study of Human Disease. Elsevier; 2017. p. 147–74. https://doi.org/10.1016/B978-0-12-809468-6.00006-1.

[2] Tsao CW, Aday AW, Almarzooq ZI, Anderson CAM, Arora P, Avery CL, et al. Heart disease and stroke statistics—2023 update: a report from the American Heart Association. Circulation 2023;147. https://doi.org/10.1161/CIR.0000000000001123.

[3] Saxton A, Tariq MA, Bordoni B. Anatomy, Thorax, Cardiac Muscle. Statpearls [Internet]. StatPearls Publishing; 2023.

[4] Degerli A, Kiranyaz S, Hamid T, Mazhar R, Gabbouj M. Early myocardial infarction detection over multi-view echocardiography. Biomed Signal Process Control 2024;87:105448.

[5] Thygesen K, Alpert JS, White HD. Universal definition of myocardial infarction. Circulation 2007;116:2634–53. https://doi.org/10.1161/CIRCULATIONAHA.107.187397.

[6] Pozo E, Sanz J. Imaging techniques in the evaluation of post-infarction function and scar. Revista Española de Cardiología (English Edition) 2014;67:754–64. https://doi.org/10.1016/j.rec.2014.04.009.

[7] Feigenbaum H. Role of echocardiography in acute myocardial infarction. Am J Cardiol 1990;66:H17–22.

[8] Cameli M, Mandoli GE, Sciaccaluga C, Mondillo S. More than 10 years of speckle tracking echocardiography: still a novel technique or a definite tool for clinical practice? Echocardiography 2019;36:958–70. https://doi.org/10.1111/echo.14339.

[9] Morariu V.I., Arnautu D.A., Morariu S.I., Popa A.M. 2D speckle tracking: a diagnostic and prognostic tool of paramount importance. 2022.

[10] Lang RM, Badano LP, Mor-Avi V, Afilalo J, Armstrong A, Ernande L, et al. Recommendations for cardiac chamber quantification by Echocardiography in adults: an update from the American Society of Echocardiography and the European Association of Cardiovascular Imaging. J Am Soc Echocardiogr 2015;28:1–39. https://doi.org/10.1016/j.echo.2014.10.003. e14.

[11] Kiranyaz S, Degerli A, Hamid T, Mazhar R, Ahmed REF, Abouhasera R, et al. Left ventricular wall motion estimation by active polynomials for acute myocardial infarction detection. IEEE Access 2020;8:210301–17.

[12] Smiseth OA, Torp H, Opdahl A, Haugaa KH, Urheim S. Myocardial strain imaging: how useful is it in clinical decision making? Eur Heart J 2016;37:1196–207. https://doi.org/10.1093/eurheartj/ehv529.

[13] Marzola F, van Alfen N, Salvi M, De Santi B, Doorduin J, Meiburger KM. Automatic segmentation of ultrasound images of gastrocnemius medialis with different echogenicity levels using convolutional neural networks. In: 2020 42nd Annual International Conference of the IEEE Engineering in Medicine & Biology Society (EMBC). IEEE; 2020. p. 2113–6.

[14] Meiburger KM, Salvi M, Giacchino M, Acharya UR, Minetto MA, Caresio C, et al. Quantitative analysis of patellar tendon abnormality in asymptomatic professional "Pallapugno" players: a texture-based ultrasound approach. Appl Sci 2018;8:660.

[15] Minetto MA, Caresio C, Salvi M, D'Angelo V, Gorji NE, Molinari F, et al. Ultrasound-based detection of glucocorticoid-induced impairments of muscle mass and structure in Cushing's disease. J Endocrinol Invest 2018. https://doi.org/10.1007/s40618-018-0979-9.

[16] Leclerc S, Smistad E, Pedrosa J, Østvik A, Cervenansky F, Espinosa F, et al. Deep learning for segmentation using an open large-scale dataset in 2D echocardiography. IEEE Trans Med Imaging 2019;38:2198–210.

[17] Degerli A, Zabihi M, Kiranyaz S, Hamid T, Mazhar R, Hamila R, et al. Early detection of myocardial infarction in low-quality echocardiography. IEEE Access 2021;9:34442–53.

[18] Nguyen T, Nguyen P, Tran D, Pham H, Nguyen Q, Le T, et al. Ensemble learning of myocardial displacements for myocardial infarction detection in echocardiography. Front Cardiovasc Med 2023;10:1185172.

[19] Hamila O, Ramanna S, Henry CJ, Kiranyaz S, Hamila R, Mazhar R, et al. Fully automated 2D and 3D convolutional neural networks pipeline for video segmentation and myocardial infarction detection in echocardiography. Multimed Tools Appl 2022;81:37417–39.

[20] Sabia P, Afrookteh A, Touchstone DA, Keller MW, Esquivel L, Kaul S. Value of regional wall motion abnormality in the emergency room diagnosis of acute myocardial infarction. A prospective study using two-dimensional echocardiography. Circulation 1991;84:I85–92.

[21] Rácz I, Fulop L, Kolozsvári R, Szabó GT, Bódi A, Péter A, et al. Wall motion changes in myocardial infarction in relation to the time elapsed from symptoms until revascularization. Anatolian J Cardiol 2015;15:363–70. https://doi.org/10.5152/akd.2014.5457.

[22] Antonelli L, Katz M, Bacal F, Makdisse MRP, Correa AG, Pereira C, et al. Heart failure with preserved left ventricular ejection fraction in patients with acute myocardial infarction. Arq Bras Cardiol 2015. https://doi.org/10.5935/abc.20150055.

[23] van Woerden G, van Veldhuisen DJ, Manintveld OC, van Empel VPM, Willems TP, de Boer RA, et al. Epicardial adipose tissue and outcome in heart failure with mid-range and preserved ejection fraction. Circ Heart Fail 2022;15. https://doi.org/10.1161/CIRCHEARTFAILURE.121.009238.

[24] Suma S. What is global longitudinal strain and its clinical importance? 2021.

[25] Zuiderveld K. Contrast limited adaptive histogram equalization. Graphics Gems 1994:474–85.

[26] Lee TC, Kashyap RL, Chu CN. Building skeleton models via 3-D medial surface axis thinning algorithms. CVGIP: Graph Models Image Process 1994;56:462–78. https://doi.org/10.1006/CGIP.1994.1042.

[27] Cerqueira MD, Weissman NJ, Dilsizian V, Jacobs AK, Kaul S, Laskey WK, et al. Standardized myocardial segmentation and nomenclature for tomographic imaging of the heart. Circulation 2002;105:539–42. https://doi.org/10.1161/hc0402.102975.

[28] Azez M. Stress echocardiography and echo in cardiopulmonary testing. Thoracic Key 2018.

[29] Joseph G, Zaremba T, Johansen MB, Ekeloef S, Heiberg E, Engblom H, et al. Echocardiographic global longitudinal strain is associated with infarct size assessed by cardiac magnetic resonance in acute myocardial infarction. Echo Res Pract 2019;6:81–9. https://doi.org/10.1530/ERP-19-0026.

[30] Lundberg S., Lee S-I.A Unified approach to interpreting model predictions 2017.

[31] Lang RM, Badano LP, Mor-Avi V, Afilalo J, Armstrong A, Ernande L, et al. Recommendations for cardiac chamber quantification by echocardiography in adults: an update from the American Society of Echocardiography and the European Association of Cardiovascular Imaging. Eur Heart J Cardiovasc Imaging 2015;16:233–71.

[32] Joseph G, Zaremba T, Johansen MB, Ekeloef S, Heiberg E, Engblom H, et al. Echocardiographic global longitudinal strain is associated with infarct size assessed by cardiac magnetic resonance in acute myocardial infarction. Echo Res Pract 2019;6:81–9.

[33] Ding J, Han X. A semi-supervised approach combining image and frequency enhancement for echocardiography segmentation. IEEE Access 2024.

[34] Seoni S, Jahmunah V, Salvi M, Barua PD, Molinari F, Acharya UR. Application of uncertainty quantification to artificial intelligence in healthcare: a review of last decade (2013–2023). Comput Biol Med 2023:107441.